ELSEVIER

Journal of Chromatography A, 947 (2002) 185–193

JOURNAL OF CHROMATOGRAPHY A

www.elsevier.com/locate/chroma

Fabrication and characterization of a rigid magnetic matrix for protein adsorption

Bo Xue, Yan Sun*

Department of Biochemical Engineering, School of Chemical Engineering and Technology, Tianjin University, Tianjin 300072, China

Received 21 September 2001; received in revised form 11 December 2001; accepted 11 December 2001

Abstract

This article describes the fabrication and characterization of a novel magnetic poly(glycidyl methacrylate–triallyl isocyanurate–divinylbenzene) matrix containing magnetite colloids. The results showed that the matrix was superparamagnetic and could be separated magnetically from a suspension in a few seconds. Protein adsorption properties of diethylamine-derivatized matrix were characterized with bovine serum albumin (BSA) as a model protein. The static capacity determined by batch adsorption was 79 mg/ml wet matrix. Kinetic study gave an effective diffusivity of BSA of $5.0 \cdot 10^{-13}$ m^2/s in the matrix at an initial BSA concentration in the liquid phase of 1.0 mg/ml. Stability of the matrix was confirmed by recycling of the matrix in protein adsorptions.

Keywords: Magnetic sorbents; Adsorption; Stationary phases, LC; Proteins; Albumin; Glycidyl methacrylate

1. Introduction

Because of their great application potentials, composite magnetic polymer matrices have been intensively investigated and employed in the fields of biotechnology and biomedicine. These include drug targeting [1], hyperthermia [2], DNA sequencing [3], cell immobilization [4] and separation [5], enzyme purification [6], and protein adsorption [7,8]. For the presently available magnetic supports used in separations of biological macromolecules, insufficient capacity and slow mass transfer kinetics are two limiting factors that restrict the applications of the supports to laboratory scales. An effective way of eliminating both the limitations at one time is to produce nano-sized, non-porous magnetic particles, so as to obtain both a relatively large surface area and fast adsorption kinetics [9]. However, to separate these particles magnetically from a suspension, a strong magnetic field with high gradient is needed to drive the particles moving against the drag force resistance. Since the high gradient makes the strength of the magnetic field attenuate rapidly with distance, the requirement of both a high field strength and a high gradient for particle separation can only be fulfilled within a very short distance from the magnetic poles [10], posing a formidable obstacle to scaling-up.

Another solution to the capacity and mass transfer problems associated with the magnetic supports is to synthesize macroporous magnetic particles with an appropriate size, usually from several to tens of micrometers. The porous structure provides a large number of inner binding sites, while the relatively small particle size and the large pores in the particles

*Corresponding author. Tel./fax: +86-22-2740-6590.
E-mail address: ysun@tju.edu.cn (Y. Sun).

0021-9673/02/$ – see front matter
PII: S0021-9673(01)01602-8

reduce the intraparticle diffusion resistance. The most attractive feature of these particles is that they need much weaker field strength and gradient in separation than the nano-sized ones, and thus are more favorable for large-scale applications.

In this work, a novel magnetic matrix is fabricated by implanting magnetite colloids onto a poly-(glycidyl methacrylate–triallyl isocyanurate–divinylbenzene) copolymer matrix, an excellent rigid medium for protein adsorption [11–13]. The matrix is fully characterized with regard to its magnetic performance and protein adsorption properties.

2. Materials and methods

2.1. Materials

Glycidyl methacrylate (GMA) (99%) was purchased from Luoyang Chenguang (Henan, China) and used without further purification. Triallyl isocyanurate (TAIC) was received from Fluka (Buchs, Switzerland). Divinylbenzene (DVB) (45% divinyl monomer) obtained from the chemical plant of Nankai University was extracted with 10% aqueous sodium hydroxide and distilled water, dried over anhydrous magnesium sulfate, and distilled under vacuum. 2,2′-Azobis-(isobutyronitrile) (AIBN) was obtained from Tianjin Dagu Chemical Factory (Tianjin, China) and recrystallized in ethanol before use. Poly(vinyl alcohol) (molecular mass 74 800–79 200, 88% hydrolyzed) was from Beijing Organic Chemical (Beijing, China). Bovine serum albumin (BSA) (fraction V, minimum 98%) was obtained from Sigma (St. Louis, MO, USA). Other reagents were all of analytical grade and used as received. A neodymium–iron–boron (NdFeB) permanent magnet manufactured by the Research Institute of Rare Earth Elements (Baotou, China) was used in solid-phase collection.

2.2. Synthesis of oleic acid-stabilized ferrofluid

Lipophilic ferrofluid was synthesized by the method of Guan et al. [14]. In 150 ml of deionized water were dissolved 7.17 g of $FeSO_4 \cdot 7H_2O$ and 14.04 g of $FeCl_3 \cdot 6H_2O$. The molar ratio of Fe^{3+} to Fe^{2+} was 2.0, so that Fe_3O_4 could be formed according to reaction stoichiometry. The solution was heated to 90 °C, to which 40 ml of 25% (w/w) $NH_3 \cdot H_2O$ was poured under vigorous agitation. A 5-ml volume of oleic acid was then added dropwise at a constant rate of 0.5 ml/min. After aging at the same temperature for 1 h, the reaction mixture was cooled to room temperature and stored in a flask for future use.

2.3. Preparation of magnetic polymer matrix

The magnetic GMA–TAIC–DVB matrix was prepared by a modification of the radical suspension copolymerization method described by Yu and Sun [11]. First, the pH of about 20 ml of the above-mentioned ferrofluid was lowered with HCl to precipitate the magnetic colloids in the ferrofluid, resulting in black magnetic slurry. Then, 1.0 g of the slurry was mixed with 20 g of GMA, 3.5 g of TAIC, 4.0 g of DVB, 7.7 g of toluene, 5.6 g of *n*-heptane and 0.5 g of AIBN. Increasing the mass of the magnetic slurry in the reaction mixture would result in higher magnetite content in the magnetic polymer matrix. The mixture was sonicated for 5 min and then transferred to a 1-l flask containing 400 ml of 1% (w/v) aqueous poly(vinyl alcohol) solution. Suspension polymerization was initiated at 45 °C with agitation (600 rpm) under a nitrogen atmosphere. The temperature of the suspension was linearly raised from 45 to 65 °C within 2 h, and was kept at 65 °C for 3 h, 75 °C for 2 h and finally 85 °C for 2 h. Brownish microbeads were formed during this course. These beads were separated magnetically from the suspension at the end of the reaction, thoroughly washed with hot water, and then extracted with ethanol in a Soxhlet extractor for at least 24 h to ensure complete removal of the porogenic solvents in the beads. With these treatments the beads were made ready for the following chemical derivatization.

2.4. Preparation of magnetic anion exchanger

A magnetic anion exchanger was prepared by immobilizing diethylamine to the magnetic GMA–TAIC–DVB (mGTD) microbeads utilizing the ring-opening reaction of the epoxide groups on the copolymer. Briefly, 5.0 g of dry beads was mixed

with 50 ml of dioxane and 50 ml of diethylamine, and the mixture was kept at 60 °C for 6 h. The modified beads were washed thoroughly with ethanol, water and finally 0.01 mol/l Tris–HCl buffer (pH 7.6) prior to protein adsorption.

2.5. Protein adsorption experiments

BSA was used as a model protein to test the adsorption characteristics of the magnetic anion exchanger. Typically, 0.05 g of drained adsorbent was mixed with 5.0 ml of buffer solution with different BSA concentrations. Unless stated otherwise, the adsorption experiments were conducted in 0.01 mol/l Tris–HCl buffer (pH 7.6) at 25 °C for 18 h in a shaking incubator. Aqueous phase ionic strength was adjusted with NaCl. At the end of adsorption, the solid phase was magnetically separated and the supernatant was analyzed for residual protein concentration. Adsorption density of BSA was calculated by mass balance.

In kinetic experiments, capped glass tubes each containing 0.05 g of drained adsorbent and 5.0 ml of BSA solution with a definite concentration were shaken end-to-end in a shaking incubator at 25 °C. The tubes were taken out successively for supernatant protein concentration measurement. By this procedure, the time course of BSA concentration decrease was determined.

2.6. Analysis and measurements

The particle size distribution (PSD) of the mGTD matrix was measured with a Mastersizer 2000 particle size analyzer (Malvern Instruments). Scanning electron microscopy (SEM) of the matrix was performed on an XL30 ESEM scanning electron microscope (Philips, The Netherlands) after sputtering gold to the sample. Information on the morphology, size and diffraction pattern of the magnetic colloids in the ferrofluid was gathered with a JEM-100CXII transmission electron microscopy (TEM) system (JEOL, Japan), and the PSD of the colloids was obtained by image analysis. The water content of the matrix was calculated from the mass loss of the matrix before and after drying [11]. Hydrated and dry particle densities were measured with a 25-ml pycnometer. The magnetization curves of dried mGTD matrices was recorded with an LDJ 9600-1 vibrating sample magnetometer (VSM) (LDJ Electronics, MI, USA), and the data were analyzed with the Langevin function to get the saturation magnetization and volumetric fraction of magnetite colloids in the matrix (see below).

BSA concentration was determined spectrophotometrically at 280 nm with an extinction coefficient of 0.608 l g^{-1} cm^{-1}.

3. Results and discussion

3.1. Properties of the magnetic matrix

Four types of mGDT matrices different mainly in their magnetite contents have been synthesized, but only the first type, Type I, is fully characterized in this work. Table 1 gives the physical properties of Type I matrix. The PSD of the magnetic beads is lognormal with a mean of 71.6 μm (Fig. 1). The shape of the beads is strictly spherical, which is observed with an optical microscope under a magnification of 100 (data not shown). The SEM graph shows the rough surface of the beads composed of numerous globules (Fig. 2), which is a typical feature of macroporous polymeric matrices [11]. Since the magnetic colloids in the matrix cannot be seen directly, those in the ferrofluid are used instead for the TEM observation. As shown in Fig. 3, the results confirm the relatively uniform size (Fig. 3a) and the crystalline nature of the colloids (Fig. 3b). The number- and volume-weighted mean diameters of the colloids are 11.6 and 14.5 nm, respectively (see Fig. 4).

Table 1
Properties of Type I magnetic matrix

d_p (μm)	ρ_h (g/ml)	ρ_d (g/ml)	w_{H_2O} (%, w/w)	ϵ_p (–)	$d_{p,m}$ (nm)
71.6	1.11	1.28	54.4	0.60[a]	14.5

[a] Calculated from the hydrated density and water content of the matrix.

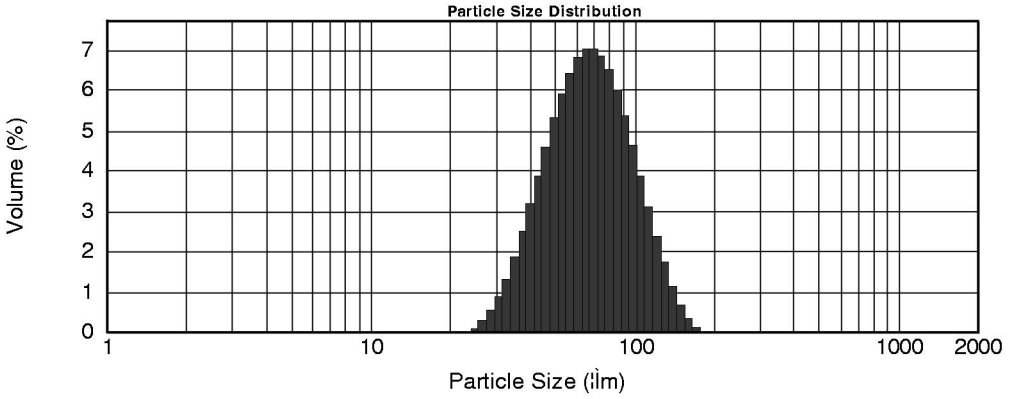

Fig. 1. Particle size distribution of mGDT beads.

3.2. Superparamagnetism

When ferromagnetic materials are divided into sufficiently small particles and dispersed in a magnetically inert environment, their magnetic behavior will change dramatically. The dispersion would be regarded as superparamagnetic rather than ferromagnetic if the following two criteria are met, that is, (a) the magnetization curve of the dispersion shows no hysteresis and (b) curves taken at different temperatures approximately superimpose when plotted against H/T [15].

The magnetization of superparamagnetic dispersions is usually described by the Langevin function [16]:

$$M = \epsilon_{\mathrm{m}} M_{\mathrm{s}} \int_0^{\infty} \left[\coth\left(\frac{\mu_0 M_{\mathrm{s}} V H}{kT} \right) - \frac{kT}{\mu_0 M_{\mathrm{s}} V H} \right] f(V)\mathrm{d}V \quad (1)$$

This function is theoretically rigorous for two kinds of dispersions: one is a fluid containing noninteracting colloids that are free to rotate with respect to the carrier fluid; the other is a solid dispersion containing colloids that are magnetically isotropic, a physically unlikely situation. In a real solid dispersion, such as the magnetic polymer matrix reported in this work, colloidal particles with magnetic anisotropy are frozen in position and form an orientation distribution of the particles' easy axes, which, if taken into account, will greatly increase the complexity and difficulty in the modeling and calculation of the magnetization of superparamagnetic systems [17]. However, neglecting these factors will not produce significant errors in most calculations, thus the Langevin function is applicable to solid dispersions in practice. Examples of such an application can be found in many publications [18,19].

Fig. 5 shows the magnetization curves of all the four types of mGDT matrices at 300 K along with the calculations from the Langevin function. No hysteresis loop is observed at this temperature, which means there would be no magnetic interactions among magnetic beads in a zero-field environment, no matter what the magnetization history of the beads is. This feature makes the dispersion of the magnetic beads easier. Low temperature magneti-

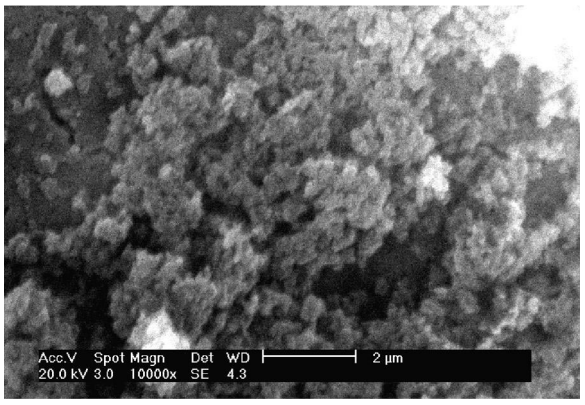

Fig. 2. Surface of mGDT matrix observed with SEM at a magnification of 10 000.

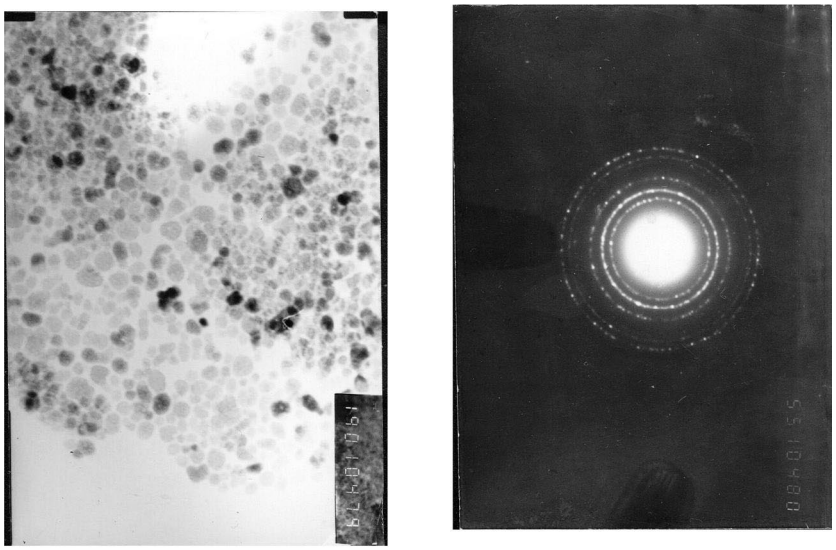

Fig. 3. Morphology and diffraction pattern of magnetite colloids in the ferrofluid. The TEM graphs were taken at magnifications of (a) 190 000 and (b) 55 000.

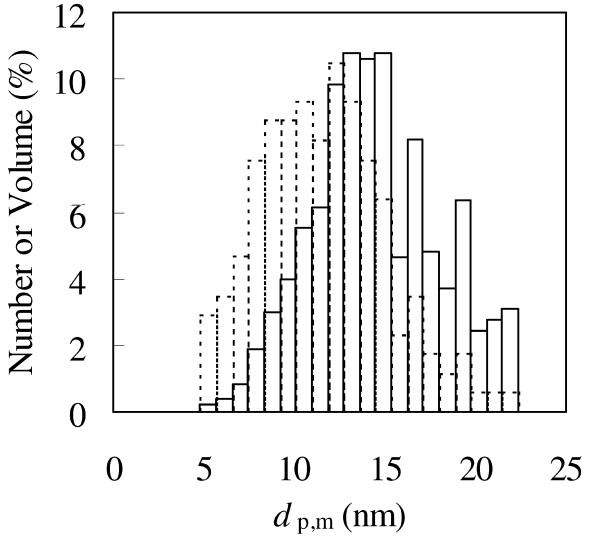

Fig. 4. Number-weighted (dashed lines) and volume-weighted (solid lines) particle size distributions of magnetite colloids obtained from the TEM graph in Fig. 3.

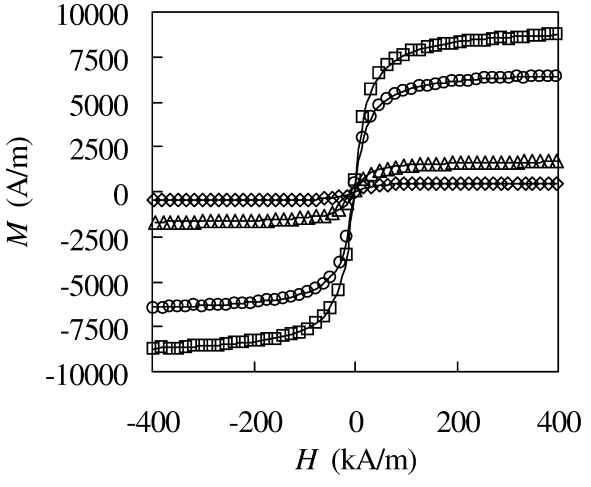

Fig. 5. Magnetization curves of mGDT matrices at 300 K. Calculations with the Langevin equation (solid lines) are in good agreement with the data measured with VSM. (◇) Type I, (△) Type II, (○) Type III, (□) Type IV. The values of M_s and ϵ_m used in the calculations are listed in Table 2.

zations of the matrices were not measured because as magnetic adsorbents for proteins, these matrices are usually used at room temperature. With only the magnetization data at one temperature, it is impossible to examine if these matrices satisfy the second criterion of superparamagnetism. Nevertheless, these matrices are considered superparamagnetic due to the fact that the largest magnetite colloids in them are less than 25 nm, a critical value below which magnetite is considered superparamagnetic [20].

3.3. Determination of M_s and ϵ_m

Given the PSD of the magnetic colloids, it is possible to estimate M_s and ϵ_m by fitting the Langevin function to the magnetization data (see Eq. (1)). This task was carried out using the large-scale algorithm for nonlinear least-squares regression provided in the optimization toolbox of MATLAB 5.3, and its results were summed up in Table 2. For all the cases studied, the saturation magnetizations are in good agreement with each other, and the correlation coefficients of the measured and calculated data are invariably larger than 99.99%. These results give a strong support to the applicability of the Langevin function to the mGDT matrices and thus provide a reliable method for determining M_s and ϵ_m. The average value of M_s is $1.75 \cdot 10^5$ A/m, about 37% that of the bulk magnetite. The reduction of M_s, reflecting a significant change in magnetic property, justifies the above conclusion that the mGDT matrices are superparamagnetic.

3.4. Efficiency in magnetic separation

Efficient separation of mGDT beads (Type I) from a suspension has been achieved in the adsorption experiments. Within less than 15 s, the beads were totally captured by the NdFeB permanent magnet, which generated a magnetic field with a maximum strength of 0.4 T and an average gradient of 5.7 T/m. This feature forms a solid basis for the potential applications of mGDT matrix in fast magnetic separation processes.

Table 2
Estimation of M_s and ϵ_m

Type of matrix	M_s ($\cdot 10^5$ A/m)	ϵ_m (%)	Correlation coefficient (%)
I	1.79	0.29	99.993
II	1.72	1.02	99.994
III	1.74	3.87	99.998
IV	1.76	5.19	99.997

3.5. Adsorption equilibrium

All the studies concerning protein adsorption have been carried out with Type I magnetic matrix. In Fig. 6 are shown the adsorption isotherms of BSA to the magnetic adsorbent. The solid lines are calculated from the Langmuir model (Eq. (2)):

$$q = \frac{q_m c}{K_d + c} \tag{2}$$

This model can be regarded as either rigorous or empirical, depending on whether the adsorption obeys its premises or not, and has been widely used in characterizing the adsorption of BSA to ion-exchange [21,22] and affinity [23] adsorbents. We choose it in this work because it is simple in form and satisfactorily accurate in correlating q and c (see Fig. 6). The values of q_m and K_d were estimated by least-squares regression. The capacity of BSA in the

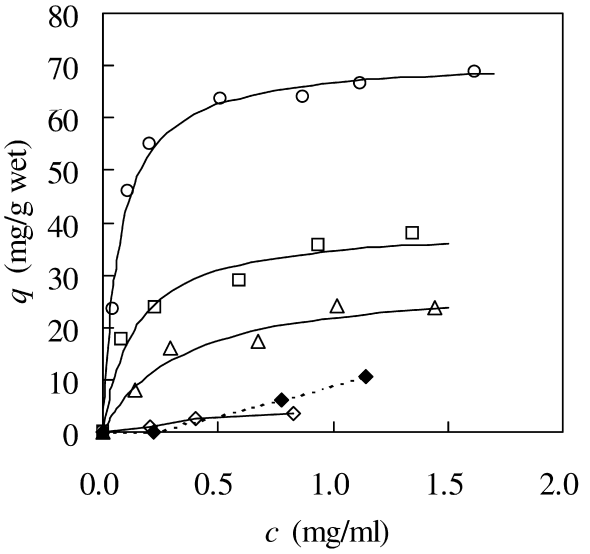

Fig. 6. Adsorption isotherms of BSA to mGDT-based anion exchanger under different aqueous phase ionic strength. NaCl concentrations (in mol/l) were (○) 0, (□) 0.1, (△) 0.2, and (◇) 0.4. Bound BSA was partly eluted from the matrix when NaCl concentration was raised from (○) 0 to (♦) 0.4.

Tris–HCl buffer without addition of NaCl was obtained at 79 mg/ml wet matrix, nearly the same as that reported in the previous work [13]. Increasing the NaCl concentration in the liquid phase can reduce the electrostatic interaction between BSA and the diethylamine groups on the matrix, suppressing the binding capacity of the adsorbent. Based on this principle, dissociation of bound BSA has been achieved, as indicated in Fig. 6.

3.6. Adsorption kinetics

A pore diffusion model is used to analyze the adsorption kinetics of BSA to the mGDT matrix [7]. The intraparticle continuity equation and its initial and boundary conditions (IC and BC) are:

$$\left(\epsilon_p + \frac{dq}{dc}\right)\cdot\frac{\partial c}{\partial t} = \frac{D_e}{r^2}\cdot\frac{\partial}{\partial r}\cdot\left(r^2\cdot\frac{\partial c}{\partial r}\right) \quad (3)$$

$$\text{IC:}\quad t = 0,\quad c = 0 \quad (3a)$$

$$\text{BC1:}\quad r = 0,\quad \frac{\partial c}{\partial r} = 0 \quad (3b)$$

$$\text{BC2:}\quad r = r_p,\quad D_e\cdot\frac{\partial c}{\partial r} = k_f\left(c_b - c|_{r=r_p}\right) \quad (3c)$$

The mass transfer of protein from liquid phase to the solid phase is written by:

$$\frac{dc_b}{dt} = -\frac{3k_f F}{r_p}\cdot\left(c_b - c|_{r=r_p}\right) \quad (4)$$

$$\text{IC:}\quad t = 0,\quad c_b = c_{b,0} \quad (4a)$$

The following correlation is used to calculate the liquid film mass transfer coefficient [24]:

$$k_f = \frac{2D_{AB}}{d_p} + 0.31\cdot\left(\frac{\mu}{\rho D_{AB}}\right)^{-2/3}\cdot\left(\frac{\Delta\rho\mu g}{\rho^2}\right)^{1/3} \quad (5)$$

Though included in the model, the external film mass transfer resistance is negligible in many practical cases, for the overall mass transfer rate of proteins to porous adsorbents is usually controlled by intraparticle diffusion [7].

The model was solved numerically, with D_e being the only adjustable parameter. Fig. 7 gives both the experimental and simulation results of adsorption kinetics under three different conditions. The D_e values obtained by data fitting are $5.0\cdot10^{-13}$ m^2/s for the first two cases ($c_{b,0}=1.0$ mg/ml) and $3.0\cdot10^{-13}$ m^2/s for the third one ($c_{b,0}=0.6$ mg/ml), indicating a positive dependence of D_e on $c_{b,0}$. The increase of D_e with $c_{b,0}$ is common for protein diffusion in ion-exchange media, and has been attributed to the enhancement of surface diffusion at higher protein concentrations [25].

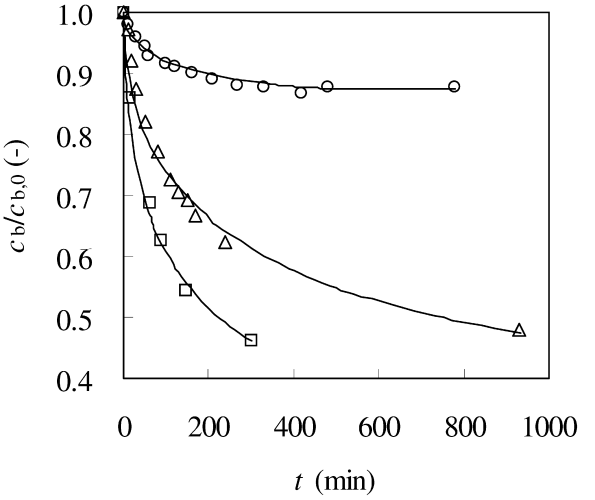

Fig. 7. Adsorption kinetics of BSA to mGDT-based anion exchanger. Experimental conditions were (○) $c_{b,0}=1.0$ mg/ml, $F=0.002$, (□) $c_{b,0}=1.0$ mg/ml, $F=0.011$, and (△) $c_{b,0}=0.6$ mg/ml, $F=0.007$. D_e values obtained by data fitting were (○) $5.0\cdot10^{-13}$ m^2/s, (□) $5.0\cdot10^{-13}$ m^2/s, and (△) $3.0\cdot10^{-13}$ m^2/s.

3.7. Recycling of the magnetic adsorbent

Repeated use of the mGDT adsorbent for BSA adsorption was investigated to test the stability of the mGDT. NaOH solution (0.1 mol/l) was employed as a regeneration agent. From Fig. 8 we know that the adsorption isotherm of BSA remains unchanged for three cycles, confirming good physical and chemical stabilities of the magnetic adsorbent at short runs. Evaluation of its long-term stability is in progress.

4. Conclusion

A novel magnetic adsorbent consisting of magnetite colloids and poly(glycidyl methacrylate–triallyl isocyanurate–divinylbenzene) copolymer was synthesized by radical suspension polymerization. The shape of the magnetization curve and the size and

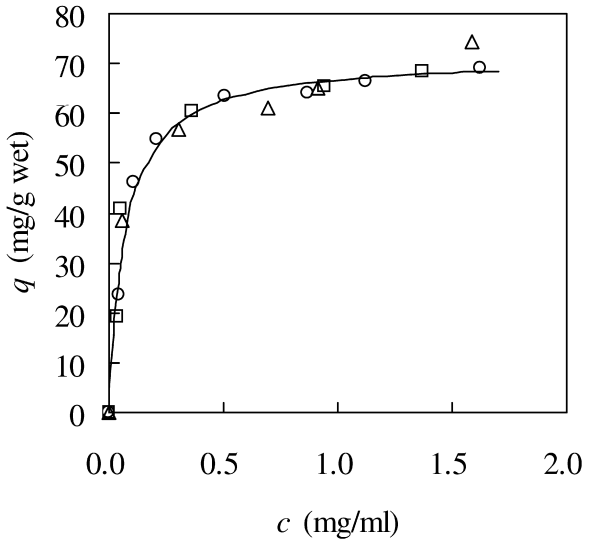

Fig. 8. Recycling of mGDT matrix. (○) Cycle 1, (□) cycle 2, (△) cycle 3.

saturation magnetization of the magnetite colloids proved the superparamagnetic nature of the matrix. With a saturation magnetization of $1.75 \cdot 10^5$ A/m and a volumetric fraction of 0.29% in dried matrix, the magnetite colloids enabled efficient magnetic separations of the magnetic beads from an aqueous suspension. Batch adsorption experiments showed that the magnetic adsorbent had a static capacity of 79 mg/ml for BSA. The effective diffusivity of BSA in the matrix depended positively on the initial BSA concentration in the liquid phase. Short-term stability of the matrix was confirmed by recycling of the matrix in batch adsorptions.

5. Nomenclature

c	Protein concentration in particle pore, mg/ml
c_b	Protein concentration in bulk liquid phase, mg/ml
$c_{b,0}$	Initial protein concentration in bulk liquid phase, mg/ml
d_p	Volume weighted mean diameter of mGDT beads, μm or m
$d_{p,m}$	Volume weighted mean diameter of magnetite colloids, nm
D_e	Effective diffusivity of protein, m^2/s
D_{AB}	Molecular diffusivity of protein, m^2/s
$f(V)$	Probability density of colloidal volume distribution, dimensionless
F	Volumetric ratio of solid phase to liquid phase, dimensionless
H	Applied magnetic field strength, A/m
k	Boltzmann's constant, $1.380662 \cdot 10^{-23}$ J/K
k_f	Liquid film mass transfer coefficient, m/s
K_d	Dissociation constant for Langmuir isotherm, mg/ml
M	Magnetization, A/m
M_s	Saturation magnetization of magnetite colloids, A/m
T	Absolute temperature, K
V	Volume of magnetite colloids, m^3
q	Adsorbed protein density, mg/ml
q_m	Adsorption capacity for Langmuir isotherm, mg/ml
r_p	Volume weighted mean radius of mGDT beads, μm or m
t	Time, min
w_{H_2O}	Water content of the matrix, % (w/w)

Greeks

ϵ_m	Volumetric fraction of magnetite colloids in the matrix, dimensionless
ϵ_p	Porosity of mGDT beads, dimentionless
μ	Liquid viscosity, kg/m/s
μ_0	Permeability in vacuum, $4\pi \cdot 10^{-7}$ H/m
ρ	Liquid density, kg/m^3
ρ_d	Density of dried mGTD beads, g/cm^3 or kg/m^3
ρ_h	Density of hydrated mGTD beads, g/cm^3 or kg/m^3
$\Delta\rho$	Density difference between hydrated matrix and liquid phase, kg/m^3

Acknowledgements

This work was supported by the National Natural Science Foundation of China (grant No. 20025617).

References

[1] S.R. Rudge, T.L. Kurtz, C.R. Vessely, L.G. Catterall, D.L. Williamson, Biomaterials 21 (2000) 1411.
[2] M. Shinkai, M. Suzuki, S. Iijima, T. Kobayashi, Biotechnol. Appl. Biochem. 21 (1994) 125.
[3] T. Hultman, M. Murby, S. Stahl, E. Hornes, M. Uhlen, Nucl. Acids Res. 18 (1990) 5107.
[4] T. Bahar, S.S. Celebi, Enzyme Microb. Technol. 26 (2000) 28.
[5] K.M. Partington, E.J. Jenkinson, G. Anderson, J. Immunol. Methods 223 (1999) 195.
[6] X.D. Tong, B. Xue, Y. Sun, Biotechnol. Prog. 17 (2001) 134.
[7] B. Xue, Y. Sun, J. Chromatogr. A 921 (2001) 109.
[8] B. Xue, X.D. Tong, Y. Sun, Sep. Sci. Technol. 36 (2001) 2449.
[9] H.P. Khng, D. Cunliffe, S. Davies, N.A. Turner, E.N. Vulfson, Biotechnol. Bioeng. 60 (1998) 419.
[10] G.P. Hatch, R.E. Stelter, J. Magn. Magn. Mater. 225 (2001) 262.
[11] Y.H. Yu, Y. Sun, J. Chromatogr. A 855 (1999) 129.
[12] M. Zhang, Y. Sun, J. Chromatogr. A 912 (2001) 31.
[13] X. Zhou, B. Xue, Y. Sun, Biotechnol. Prog. 17 (2001) 1093.
[14] Y.-P. Guan, H.-Z. Liu, Z.-T. An, J.-J. Ke, J.-Y. Chen, CN Pat. 1 253 147 (2000).
[15] C.P. Bean, J.D. Livingston, J. Appl. Phys. 30 (1959) 120S.
[16] R.W. Chantrell, J. Popplewell, S.W. Charles, IEEE Trans. Mag. 14 (1978) 975.
[17] R.W. Chantrell, N.Y. Ayoub, J. Popplewell, J. Magn. Magn. Mater. 53 (1985) 199.
[18] C.L. Chien, J. Appl. Phys. 69 (1991) 5267.
[19] J.K. Vassiliou, V. Mehrotra, M.W. Russell, E.P. Giannelis, R.D. McMichael, R.D. Schull, R.F. Ziolo, J. Appl. Phys. 73 (1993) 5109.
[20] J. Lee, T. Isobe, M. Senna, J. Colloid Interface Sci. 177 (1996) 490.
[21] G.L. Skidmore, B.J. Horstmann, H.A. Chase, J. Chromatogr. 498 (1990) 113.
[22] H. Yoshida, M. Yoshikawa, T. Kataoka, AIChE J. 40 (1994) 2034.
[23] L.Z. He, Y.R. Gan, Y. Sun, Bioprocess Eng. 17 (1997) 301.
[24] B.J. Horstmann, H.A. Chase, Chem. Eng. Res. Des. 67 (1989) 243.
[25] K. Miyabe, G. Guiochon, J. Chromatogr. A 866 (2000) 147.